JOURNAL OF CHEMICAL & ENGINEERING DATA

ARTICLE

pubs.acs.org/jced

Kinetics and Mechanism of the Food Dye FD&C Red 40 Adsorption onto Chitosan

Jeferson S. Piccin,[†,‡] Guilherme L. Dotto,[†] Mery L. G. Vieira,[†] and Luiz A. A. Pinto[*,†]

[†]Unit Operation Laboratory, School of Chemistry and Food, Federal University of Rio Grande-FURG, Rio Grande, RS, Brazil

[‡]Department of Chemical Engineering, Federal University of Rio Grande do Sul-UFRGS, Porto Alegre, RS, Brazil

ABSTRACT: The kinetics and mechanism of the food dye disodium 6-hydroxy-5-((2-methoxy-5-methyl-4-sulfophenyl)azo)-2-naphthalenesulfonate (FD&C Red 40) adsorption onto chitosan were studied. The effects of pH (5.7 to 7.4), chitosan dosage [(250 to 500) mg·L^{-1}], deacetylation degree (42 % to 84 %), and particle size [(0.10 to 0.26) mm] were investigated. The adsorption reaction models were used to evaluate the kinetic behavior. Infrared analysis and models based on mass transfer phenomena were used to investigate the adsorption mechanism. The maximum adsorption capacity (300 mg·g^{-1}) was found at a pH 5.7, chitosan dosage of 250 mg·L^{-1}, deacetylation degree of 84 %, and particle size of 0.10 mm. Pseudosecond-order and Elovich models were the most appropriate to fit the experimental data of adsorption kinetics. The adsorption process was controlled by intraparticle diffusion, film diffusion, or convection according to the experimental conditions. Infrared analysis showed the chemical interaction between chitosan and food dye FD&C Red 40.

INTRODUCTION

Many industries use a variety of dyes to color their products, for example, in the textile, rubber, paper, plastics, leather, cosmetics, food, and mineral processing industries.[1] The azobenzene dye disodium 6-hydroxy-5-((2-methoxy-5-methyl-4-sulfophenyl)azo)-2-naphthalenesulfonate (FD&C Red 40; Figure 1) is used in food, pharmaceutical, and cosmetics industries. There has been a increase in production and utilization of dyes in the last few decades, and because of its low fixation degree, a large amount of this dye is discharged into effluents.[2,3] The discharge of dyes into receiving waters causes extremely toxic effects to aquatic life even at low concentrations.[4] Thus, several governments have established environmental restrictions with regard to the quality of colored wastewater, and they have obligated the industries to remove dyes from their effluents before discharging.[5] Some methods are used to remove dye from effluents, such as electroflocculation, membrane filtration, electrochemical destruction, ion-exchange, irradiation, precipitation, and ozonation. However, these technologies are generally ineffective in color removal, expensive, and less adaptable to a wide range of dye wastewaters.[6] Adsorption has been studied as an alternative to treat effluents contaminated with dyes, due to an low initial investment, simplicity of project and operation, no toxicity, and higher efficiency than the conventional processes.[7]

Many alternative adsorbents to remove dye from aqueous solutions were studied in the literature, such as almond shell,[4] acai stalks,[8] palm shell powder,[9] rice husk ash,[10] fly ash,[11] date stones,[12] and sep tiolite.[13] The adsorption onto chitosan is one of the emergent methods for the dye removal. Chitosan is a cationic polysaccharide prepared from the chitin deacetylation.[7] The majority of works about dye removal onto chitosan use commercial chitosan with defined characteristics or chitosan derivates to remove textile dyes;[9,14−17] however, food dye adsorption onto chitosan with different characteristics is little investigated.[18]

Dye removal is based on various factors which include adsorbate−adsorbent relationships (interactions).[19] Kinetics and mechanism are fundamental aspects to elucidate how the interactions between adsorbent and adsorbate occur. Kinetics explains how fast the reaction occurs, and also it leads to information on the factors affecting the reaction rate. The adsorption mechanism shows the interactions occurring at the adsorbent/adsorbate interface.[7] Generally, the adsorption kinetics is described using adsorption reaction models or models based on mass transfer phenomena.[1,4,7,9,20]

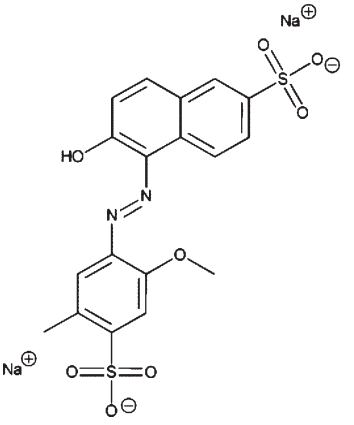

Figure 1. Chemical structure of FD&C Red 40.

In this work, the food dye FD&C Red 40 adsorption onto chitosan was studied. The effects of chitosan dosage, pH, deacetylation degree, and particle size on the adsorption kinetics and mechanism were investigated. The adsorption reaction models were used to investigate kinetic behavior. Infrared analysis and models based on mass transfer phenomena were used to determine the adsorption mechanism.

Received: April 21, 2011
Accepted: September 7, 2011
Published: September 19, 2011

Table 1. Surface Area, Average Pore Radius, and Pore Volume of Chitosan with Different Particle Sizes

	particle size (mm)		
characteristics	0.10	0.18	0.26
surface area[a] ($m^2 \cdot g^{-1}$)	4.2 ± 0.1	3.4 ± 0.1	1.6 ± 0.1
average pore radius[a] (Å)	25.1 ± 0.2	24.2 ± 0.2	24.7 ± 0.2
pore volume[a] ($mm^3 \cdot g^{-1}$)	9.5 ± 0.1	4.8 ± 0.1	2.1 ± 0.1

[a] Mean ± standard error, in triplicate.

EXPERIMENTAL SECTION

Adsorbate. The commercial food dye FD&C Red 40 ($C_{18}H_{14}N_2O_8S_2Na_2$, molecular weight 496.4 $g \cdot mol^{-1}$, C.I. 16045, λ_{max} = 500 nm, pK_a = 11.4, chemical structure shown in Figure 1) was supplied by a local manufacturer, Plury Chemical Ltd., with a purity higher than 85 %. All other reagents were of analytical grade. Distilled water was used to prepare all solutions.

Chitosan Production and Characterization. First, chitin was obtained from shrimp (*Farfantapenaeus brasiliensis*) wastes by demineralization, deproteinization, and deodorization steps.[21]

The chitin deacetylation was carried out at 403 K in a reactor under heating and agitation (50 rpm), where 2 L of sodium hydroxide solution (0.425 $kg \cdot L^{-1}$) were added to 30 g of chitin. The reaction times were (5, 25, and 100) min, to result in (42, 64, and 84) % of the deacetylation degree, respectively.[22] Chitosan samples obtained were purified,[21] dried,[23] and sieved until the particle sizes of (0.10 ± 0.02, 0.18 ± 0.02, and 0.26 ± 0.02) mm. The deacetylation degree was determined by Fourier transform infrared (FT-IR) analysis[24] (Prestige 21, the 210045, Japan), and the molecular weight of chitosan was determined by an intrinsic viscosity method.[21] In addition, chitosan with different particle sizes was characterized in relation to the surface area, average pore radius, and pore volume through the BET method[3] (Quantachrome, Nova station A, USA). The chitosan molecular weight was 145 ± 3 kDa. The results of the Brunauer–Emmett–Teller (BET) analysis are presented in Table 1.

Batch Adsorption Experiments. In this study the effects of chitosan dosage [(250, 375, and 500) $mg \cdot L^{-1}$ of the powder sample], pH (5.7, 6.6, and 7.4), deacetylation degree [(42 ± 5, 64 ± 3, and 84 ± 3) %], and particle size [(0.10 ± 0.02, 0.18 ± 0.02, and 0.26 ± 0.02) mm] were investigated.

Chitosan powder samples were added in 0.8 L of distilled water, and its pH was corrected for the study conditions through the 50 mL addition of buffer dissodic phosphate/citric acid (0.1 $mol \cdot kg^{-1}$), which did not present interactions with the dye. The solutions were stirred for 30 min until pH reached the equilibrium, and the pH was measured before and after the adsorption process by a pH meter (Mars, MB10, Brazil). The potentiometric cell for pH measurements consists in a glass electrode and a thermometer connected in a signal processor. The calibration of the glass electrode was carried out using buffers supplied by the Mars Company. A solution (50 mL) with 2 $g \cdot L^{-1}$ of dye concentration was added to each chitosan solution, and it was completed to 1 L with distilled water, so that the initial concentration of dye was approximately 100 $mg \cdot L^{-1}$ in all solutions.[18,20,25]

Adsorption experiments were carried out in jar test (Miller, JP101, Brazil), under constant agitation of 100 rpm and ambient temperature (298 ± 1 K). Aliquots were removed in preset time intervals [(2, 4, 6, 8, 10, 15, 20, 25, 30, 40, 50, 60, 80, 100, and 120) min] through filtration with Whatmann Filter Paper No. 40, which did not present interaction with the dye. The dye concentration was determined by spectrophotometry (Quimis, Q108 DRM, Brazil) at 500 nm (the maximum wavelength of the dye is not influenced by the pH value). Each kinetics experiment was carried out in duplicate, and blanks (dye solutions without adsorbent) were carried out in all experiments. The adsorption capacity (q_t) was determined by eq 1:

$$q_t = \frac{C_0 - C_t}{m} V \tag{1}$$

where C_0 is the initial dye concentration in liquid phase ($mg \cdot L^{-1}$), C_t is the dye concentration in liquid phase at time t ($mg \cdot L^{-1}$), m is the adsorbent amount (g), and V is the volume of solution (L).

Kinetic Models. The pseudofirst-order and pseudosecond-order kinetic models assume that the adsorption is a pseudochemical reaction, and the adsorption rate can be determined, respectively, for the pseudofirst-order, eq 2, and pseudosecond-order, eq 3 equations:[26]

$$q_t = q_1(1 - \exp(-k_1 t)) \tag{2}$$

$$q_t = \frac{t}{(1/k_2 q_2^2) + (t/q_2)} \tag{3}$$

where k_1 and k_2 are the kinetic coefficients of the pseudofirst and pseudosecond order (min^{-1} and $g \cdot mg \cdot min^{-1}$), respectively, and q_1 and q_2 are the theoretical values for the adsorption capacity ($mg \cdot g^{-1}$) found through the pseudofirst- and pseudosecond-order models, respectively.

When the adsorption processes involve chemisorption in the solid surface and the adsorption rate decreases with the time due to covering of the superficial layer, the Elovich model, eq 4, is one of the most used.[27]

$$q_t = \frac{1}{a}\ln(1 + abt) \tag{4}$$

where a is considered the initial rate due to $(dq/dt) = a$ with $q_t = 0$ ($mg \cdot g^{-1} \cdot min^{-1}$) and b is the desorption constant of the Elovich model ($g \cdot mg^{-1}$).

The kinetic coefficient values were determined from the fit of the models to the experimental data through no linear regression by software Statistic 6.0 (Statsoft, USA). The fit quality was verified through the coefficient of determination (R^2) and average relative error (E), eq 5:[18,20,25]

$$E = \frac{100}{n}\sum_{1}^{n}\frac{|q_{t,\exp} - q_{t,\mathrm{obs}}|}{q_{t,\mathrm{obs}}} \tag{5}$$

where $q_{t,exp}$ and $q_{t,obs}$ are, respectively, the experimental value and calculated value of adsorption capacity in time t.

Mechanism Models. The physical-chemical nature of the adsorbate and adsorbent can affect external and internal diffusion of the adsorption process.[28]

In the case of external convection, the model assumes that, for short times, the diffusion step does not affect the adsorption rate.[28] The model can be described by eq 6:

$$\frac{q_t}{q_e} = \frac{C_o}{C_o - C_e}\left(1 - \exp\left(-k_f \frac{A}{V} t\right)\right) \tag{6}$$

where (q_t/q_e) is the relation between the adsorption capacity and the equilibrium adsorption and can be interpreted as the

Table 2. Kinetic Parameters for the Adsorption of FD&C Red 40 by Chitosan

	pseudofirst order				pseudosecond order				Elovich model				
	k_1	q_1		E	$10^4\ k_2$	q_2		E	a	b		E	calcd q_e
effect	min^{-1}	$mg \cdot g^{-1}$	R^2	%	$g \cdot mg^{-1} \cdot min^{-1}$	$mg \cdot g^{-1}$	R^2	%	$mg \cdot g^{-1} \cdot min^{-1}$	$g \cdot mg^{-1}$	R^2	%	$mg \cdot g^{-1}$
Chitosan Dosage (pH = 6.6; DD = 84 ± 3 %; d = 0.10 ± 0.02 mm)													
250 $mg \cdot L^{-1}$	0.070	166.1	0.93	13.8	4.59	191.6	0.97	8.3	0.025	35.1	0.99	2.5	314.3
375 $mg \cdot L^{-1}$	0.073	153.1	0.94	12.8	5.13	176.8	0.98	7.2	0.027	33.2	0.99	1.2	236.3
500 $mg \cdot L^{-1}$	0.087	150.4	0.93	12.4	6.51	171.5	0.97	6.9	0.03	45.7	0.99	1.3	183.6
pH (m = 250 $mg \cdot L^{-1}$; DD = 84 ± 3 %; d = 0.10 ± 0.02 mm)													
5.7	0.472	277.1	0.94	6.3	24.62	299.2	0.99	3.2	0.029	4770.2	0.99	2.1	296.2
6.6	0.070	166.1	0.93	13.8	4.59	191.6	0.97	8.3	0.025	35.1	0.99	2.5	314.3
7.4	0.084	65.4	0.96	9.3	14.86	74.1	0.97	6.5	0.069	19.3	0.98	6.2	70.8
Deacetylation Degree (m = 250 $mg \cdot L^{-1}$; pH = 6.6; d = 0.10 ± 0.02 mm)													
42 ± 5 %	0.046	147.2	0.95	13.2	2.88	177.4	0.98	7.6	0.023	14.2	0.99	4.3	227.7
64 ± 3 %	0.036	156.1	0.97	12.5	1.90	184.0	0.99	8.9	0.02	10.4	0.99	4.5	240.8
84 ± 3 %	0.070	166.1	0.93	13.8	4.59	191.6	0.97	8.3	0.025	35.1	0.99	2.5	314.3
Particle Size (m = 250 $mg \cdot L^{-1}$; pH = 6.6; DD = 84 ± 3 %)													
0.10 ± 0.02 mm	0.070	166.1	0.93	13.8	4.59	191.6	0.97	8.3	0.025	35.1	0.99	2.5	314.3
0.18 ± 0.02 mm	0.043	128.2	0.98	8.9	2.84	157.5	0.99	3.8	0.025	10.3	0.99	3.2	235.5
0.26 ± 0.02 mm	0.033	84.5	0.94	17.6	3.32	104.9	0.97	13	0.036	5.2	0.98	7.9	183.4

saturation adsorbent rate, C_e is the concentration in the liquid phase at equilibrium ($mg \cdot g^{-1}$), k_f is the external convection coefficient ($m \cdot s^{-1}$), and A/V is the volumetric area of the particle (m^{-1}).

Crank[29] presented solutions of models based on the Fick law for the diffusion in the boundary layer between adsorbent and the solution (eq 7) and for the internal particle diffusion (eq 8):

$$\frac{q_t}{q_e} = 6\left(\frac{D_f}{\pi {R_p}^2}\right)^{0.5} t^{0.5} \tag{7}$$

$$\frac{q_t}{q_e} = 1 - \exp\left(\ln\left(\frac{6}{\pi^2}\right) - \left(\frac{D_p \pi^2}{{R_p}^2} t\right)\right) \tag{8}$$

where D_f and D_p are the external and internal diffusivity coefficients ($m^2 \cdot s^{-1}$) and R_p is the average radius of the adsorbent particle (m).

The values of k_f, D_f, and D_p were calculated by fit of eqs 6 to 8 to the experimental data through an interactive process. The model that presented the lower value of relative error was considered the one that controlled the process during the time interval; the average value of the considered relative error was minimized using the tool Solver of Microsoft Excel.

The evaluation of the influence of each mechanism on the dye adsorption resistance was found by a nondimensional Biot number (N_{Bi}), which is the relation between the resistances to the convection and the diffusion,[30] and it was calculated from eq 9:

$$N_{Bi} = \frac{k_f d C_0}{2 \rho_a D_p q_0} \tag{9}$$

where d is the particle size (m), ρ_a is the adsorbent density ($kg \cdot m^{-3}$), and q_0 is the adsorption capacity ($mg \cdot g^{-1}$) considering $C_e = C_0$.

FT-IR Analysis. To verify chitosan−dye interactions, FT-IR analysis was carried out in the more adequate conditions of the adsorption process. Chitosan samples before and after the adsorption were dried (378 K) until constant weight. After this, the samples were macerated and carried out in the spectroscopic determination in the region of the infrared ray (Prestige 21, the 210045, Japan), using the technique of diffuse reflectance in potassium bromide.[31]

RESULTS AND DISCUSSION

Adsorption Kinetics. Table 2 shows the calculated parameter values of the pseudofirst-order, pseudosecond-order, and Elovich models and its respective coefficient of determination and the average relative error values, for different chitosan dosages (m), pH, deacetylation degree (DD), and particle size (d).

In Table 2, the coefficient of determination ($R^2 > 0.97$) and the average relative error ($E < 10$ %) of the pseudosecond-order and Elovich models shows that these models were satisfactory to represent the experimental data. This suggests that the adsorption of FD&C Red 40 onto chitosan occurred through internal and external mass transfer and chemisorption was an important step in process. Similar results were found by other researchers, in basic dye adsorption onto the almond shell[4] and in the adsorption of acid blue 9 and food yellow 3 onto chitosan.[20]

The theoretical adsorption capacity values of the pseudofirst- and pseudosecond-order models, q_1 and q_2, in Table 2, show that both of the models underestimate this parameter when compared with the values calculated from the experimental adsorption isotherms, q_e (Table 2). This shows that both models were not capable to represent the experimental data until the end of the adsorption.

The effects of chitosan dosage, pH, deacetylation degree, and particle size on FD&C Red 40 adsorption kinetics were shown in Figures 2, 3, 4, and 5, respectively.

dx.doi.org/10.1021/je200388s |J. Chem. Eng. Data 2011, 56, 3759–3765

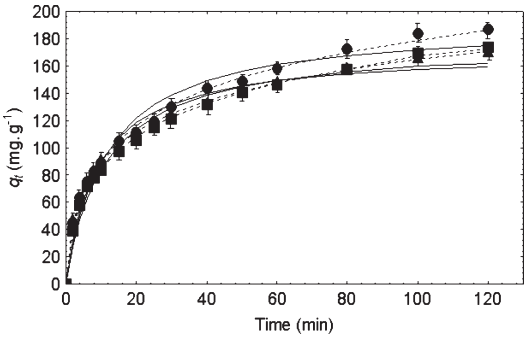

Figure 2. Chitosan dosage effect on the adsorption kinetics of food dye FD&C Red 40: ●, m = 250 mg·L^{-1}; ■, m = 375 mg·L^{-1}; ▲, m = 500 mg·L^{-1}; —, pseudosecond-order model; - - -, Elovich model.

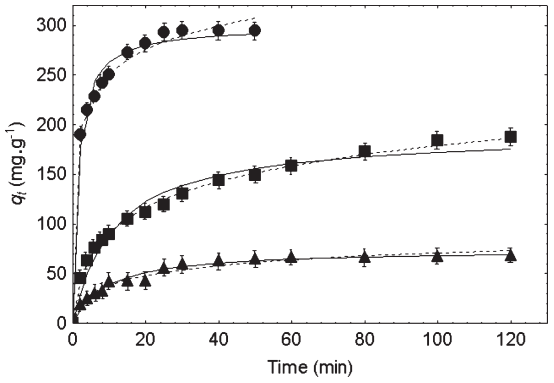

Figure 3. pH effect on the adsorption kinetics of food dye FD&C Red 40: ●, pH 5.7; ■, pH 6.6; ▲, pH 7.5; —, pseudosecond-order model; - - -, Elovich model.

Chitosan Dosage Effect. The chitosan dosage effect did not present a difference in the adsorption capacity in the first half-hour; however, after this time the increase in chitosan dosage leads to a decrease in adsorption capacity (Figure 2). This behavior can be explained due to the aggregation of adsorption sites; that is, it results in a decrease in total area available of the adsorbent surface to the dye and an increase in diffusion path length.[12] Other researchers showed that the increase in the amount of aqai stalks caused a large decrease in the adsorption capacity of Reactive Black 5 and Reactive Orange 16.[8]

pH Effect. Figure 3 shows that the pH decrease is caused by a large increase in the adsorption capacity of FD&C Red 40. In acid pH (5.7) the amino group of chitosan is protonated to form $-NH_3^+$, leading to repulsion between the polymeric chains and increasing the solubility in the solution. In this way, the protonated amine attracts the sulfonated group of the dye, that in solution is $-SO_3^-$, and the adsorption occurs through an electrostatic interaction. On the other hand, in alkaline conditions of pH (7.4), the amino groups are not protonated, and the interaction between the dye and the adsorbent occurs by van der Waals forces. The adsorption occurs preferentially for physical interaction, decreasing the adsorption capacity. Other researchers[25] found that the adsorption capacity of the dye acid blue 9 by chitosan decreases approximately from (219 to 87) mg·g^{-1} with the increase of pH from 3 to 5.

Deacetylation Degree Effect. Figure 4 shows no verified alteration in the adsorption capacity due to the increase of the deacetylation degree from (42 ± 5 to 64 ± 3) % in the

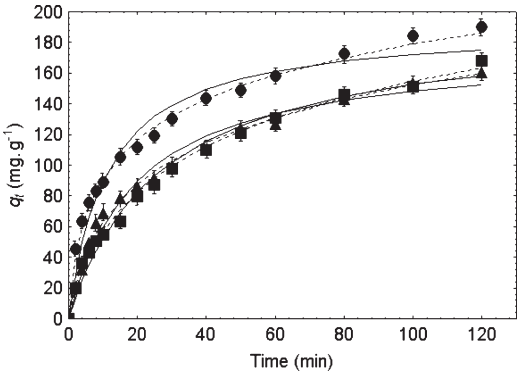

Figure 4. Chitosan deacetylation degree effect on the adsorption kinetics of food dye FD&C Red 40: ▲, DD = 42 ± 5 %; ■, DD = 64 ± 3 %; ●, DD = 84 ± 3 %; —, pseudosecond-order model; - - -, Elovich model.

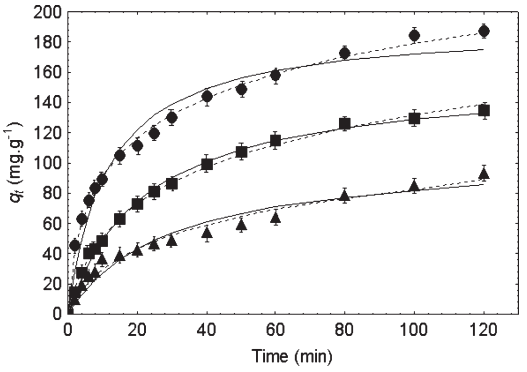

Figure 5. Particle size effect on adsorption kinetics of food dye FD&C Red 40: ●, d = 0.10 ± 0.02 mm; ■, d = 0.18 ± 0.02 mm; ▲, d = 0.26 ± 0.02 mm; —, pseudosecond-order model; - - -, Elovich model.

experimental time, but an increase from (64 ± 3 to 84 ± 3) % increased the adsorption capacity. This behavior can be explained due to two facts: First, the increase in deacetylation degree causes a reduction in the material crystallinity; thus the material porosity increases, and it facilitates the adsorption of physical nature.[7] Second, the increase in deacetylation degree leads to an increment in the amount of available amino groups of chitosan to be protonated and thus to make chemical nature adsorption of the dye. Similar works using chitosan[31] observed that the removal of the dye Reactive Red No. 141 presented an increase from (63.9 to 81.9) % with the increase of the deacetylation degree from (48 to 90) %.

Particle Size Effect. In Figure 5 and Table 2, the adsorption capacity values increase considerably with the reduction of the particle size. This occurs because particle size reduction leads to an increment of the surface area and pore volume of the adsorbent, as shown in Table 1; consequently, more adsorption sites are exposed.[7] Similar results were obtained by other researchers.[6,7,18,19]

The kinetic study showed that the pseudosecond-order and Elovich models were satisfactory to represent all experimental data, and it indicates the chemisorption. The best adsorption capacity was 300 mg·g^{-1} obtained at pH 5.7, chitosan dosage 250 mg·L^{-1}, deacetylation degree 84 %, and particle size 0.10 mm.

Adsorption Mechanisms. Table 3 presents the values of the external convection (k_f), external diffusion (D_f), internal diffusion

Table 3. Convection, Internal, and External Diffusion Coefficient Values and Biot Number Calculated to the Adsorption of Food Dye FD&C Red 40 by Chitosan

effect	$10^4\ k_f$ / $m \cdot s^{-1}$	$10^{13}\ D_f$ / $m^2 \cdot s^{-1}$	$10^{13}\ D_p$ / $m^2 \cdot s^{-1}$	N_{Bi}
Chitosan Dosage (Sample Powder) (pH = 6.6; DD = 84 ± 3 %; d = 0.10 ± 0.02 mm)				
250 $mg \cdot L^{-1}$	7.56	2.87	1.40	46.4
375 $mg \cdot L^{-1}$	6.62	4.81	3.08	18.5
500 $mg \cdot L^{-1}$	8.23	8.88	8.27	8.6
pH (Dosage = 250 $mg \cdot L^{-1}$; DD = 84 ± 3 %; d = 0.10 ± 0.02 mm)				
5.7	74.71	62.12	61.80	11.1
6.6	7.56	2.87	1.40	46.4
7.4	2.91	9.05	16.43	5.1
Deacetylation Degree (DD) (Dosage = 250 $mg \cdot L^{-1}$; DD = 84 ± 3 %; d = 0.10 ± 0.02 mm)				
42 ± 5 %	3.74	2.30	2.56	17.9
64 ± 3 %	4.08	1.86	2.22	20.0
84 ± 3 %	7.56	2.87	1.40	46.4
Particle Size (d) (Dosage = 250 $mg \cdot L^{-1}$; pH = 6.6; DD = 84 ± 3 %)				
0.10 ± 0.02 mm	7.56	2.87	1.40	46.4
0.18 ± 0.02 mm	6.33	3.68	2.81	30.1
0.26 ± 0.02 mm	5.37	5.97	4.80	40.0

(D_p) coefficients, and the Biot number (N_{Bi}) of the models based in the mass transfer mechanisms for the adsorption of the food dye FD&C Red No. 40 by chitosan under different conditions.

Table 3 shows that the external convection coefficient (k_f) values decreased with the increase of pH from 5.7 to 7.5. The internal diffusion coefficients (D_p) presented lower values at pH 6.6. The external diffusion coefficients (D_f) were higher than the internal (D_p) values only at neutral pH. The behaviors of the mass transfer mechanisms showed that 70 % of the chitosan saturation was reached in the first 20 min of the adsorption process for pH values from 5.7 to 7.5. In these conditions, the mechanisms that had controlled the adsorption process were the convection for acid pH and the film diffusion in neutral pH. The first fact can be explained by the protonation of chitosan that leads to the repulsion of the polymeric chains, increasing the solubility in the solution and changing the adsorption area. In neutral conditions, the interaction between the dye and chitosan occurs by van der Waals forces, and the adsorption occurs preferentially for physical interaction.[7] The decrease of the internal diffusive effect on the adsorption mechanism in these conditions can be observed by the low values of the Biot number. At the pH of 6.6, the diffusive mechanism presented an increase of the resistance on the adsorption process, and it leads to an increase in the Biot number. In a range of pH between 6.5 and 6.7, all chitosan amino groups are protonated; however, the repulsion of the polymer chains only occurs with pH lower than 6.5, and the adsorption occurs in the interior of the particle.[7]

The effect of the deacetylation degree on the coefficient values in Table 3 shows a decrease in the resistance to the mass transfer due to convection with the increase of the deacetylation degree, which can be observed by the increase of the convection coefficient values. However, when the internal diffusion starts to take control, the process has an inverse effect of the deacetylation degree on the resistance to the adsorption process; therefore, the values of D_p for the deacetylation degree of 84 ± 3 % were almost two times lower. The predominance of the diffusive mechanism on the control of the adsorption process can be verified by the increase of the Biot number with the increase of the deacetylation degree.

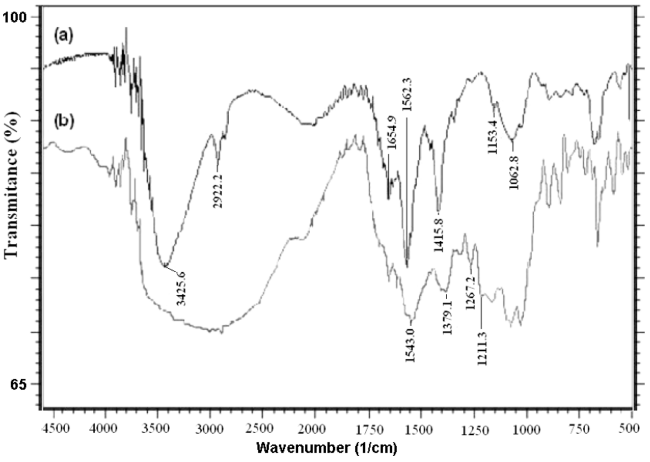

Figure 6. FT-IR analysis of chitosan: (a) before adsorption process; (b) chitosan saturated with food dye FD&C Red 40.

In Table 3 a decrease in the convection resistance with increasing particle size is observed. The external and internal diffusion coefficients had a constant increase with increments of the particle size. The Biot number demonstrates that the increase of the adsorption capacity due to the reduction of the particle size occurs, in its majority, because of the formation of a thick dye layer on the chitosan surface, and the increment of the particle size leads to an increase of the necessary time so that the equilibrium occurs.

Figure 6 shows FT-IR analysis of chitosan in acid conditions, and it was carried out before and after the adsorption process.

dx.doi.org/10.1021/je200388s |J. Chem. Eng. Data 2011, 56, 3759–3765

Figure 6 (curve a) shows the bands 3425.6 cm^{-1} of OH linked to a structure of chitosan. The bands of 1062.8 cm^{-1} indicate the stretching of linking C−O−C presents in the existing cycle on the chitosan molecule. The stretching of primary amine linking N−H, characteristic of chitosan, meets in the band of 2922.2 cm^{-1}. The amine deformation can be observed in the bands of (1562.3 and 1415.8) cm^{-1}. However, after the adsorption process in acid conditions, Figure 6 (curve b), it is possible to observe the bands of (1267.2 and 1211.3) cm^{-1} corresponding to the stretching of aromatic rings and the sulfonated groupings presented in the dye structure, respectively. Besides, the bands on (1562.3 and 1415.8) cm^{-1} are modified to the bands on (1543.0 and 1379.1) cm^{-1} due to the electrostatic interaction between the amine protonated group of chitosan ($-NH_3^+$) and sulfonated group of dye ($-SO_3^-$) that leads to the chemical nature of the adsorption process.

The mechanism study showed that the adsorption of FD&C Red 40 onto chitosan was strongly dependent on experimental conditions and chitosan characteristics. The process may be controlled by intraparticle diffusion, film diffusion, or convection, depending on the experimental conditions. In the best conditions, adsorption process was controlled by convection, and chemisorption was observed.

CONCLUSION

The present investigation showed that, in all conditions, adsorption kinetics followed pseudosecond-order and Elovich models ($R^2 > 0.97$ and $E\% < 10$ %) suggesting that chemisorption and internal and external mass transfer mechanisms were important factors in the adsorption process.

It was verified that the decrease in the chitosan dosage, pH, and the particle size and increase of the deacetylation degree leads to an increase in adsorption capacity. The best result (300 $mg \cdot g^{-1}$) was found in the following conditions: chitosan dosage of 250 $mg \cdot L^{-1}$ of powder sample, pH of 5.7, deacetylation degree of 84 ± 3 %, and particle size of 0.10 ± 0.02 mm. In these conditions, adsorption process was controlled by a convection mechanism; however, in other conditions it was verified that the limiting step in the adsorption rate was the film or intraparticle diffusion. Through FT-IR analysis, it was possible to verify the chemical nature of the adsorption process.

AUTHOR INFORMATION

Corresponding Author

*Mailing address: FURG, 475 Engenheiro Alfredo Huch Street, 96201-900, Rio Grande, RS, Brazil. Tel.: +55 53 3233 8645. Fax: +55 53 3233 8745. E-mail address: dqmpinto@furg.br.

Funding Sources

The authors would like to thank CAPES (Brazilian Agency for Improvement of Graduate Personnel) and CNPq (National Council of Science and Technological Development) for financial support.

REFERENCES

(1) Atar, N.; Olgun, A.; Wang, S.; Liu, S. Adsorption of Anionic Dyes on Boron Industry Waste in Single and Binary Solutions Using Batch and Fixed-Bed Systems. *J. Chem. Eng. Data* **2011**, *56*, 508–516.

(2) Salem, M. A.; Al-Ghonemiy, A. F.; Zaki, A. B. Photocatalytic degradation of Allura red and Quinoline yellow with Polyaniline/TiO_2 nanocomposite. *Appl. Catal., B* **2009**, *91*, 59–66.

(3) Iriarte-Velasco, U.; Chimeno-Alanís, N.; Gonzalez-Marcos, M. P.; Alvarez-Uriarte, J. I. Relationship between Thermodynamic Data and Adsorption/Desorption Performance of Acid and Basic Dyes onto Activated Carbons. *J. Chem. Eng. Data* **2011**, *56*, 2100–2109.

(4) Duran, C.; Ozdes, D.; Gundogdu, A.; Senturk, H. B. Kinetics and Isotherm Analysis of Basic Dyes Adsorption onto Almond Shell (*Prunus dulcis*) as a Low Cost Adsorbent. *J. Chem. Eng. Data* **2011**, *56*, 2136–2147.

(5) Mahmoodi, N. M.; Hayati, B.; Arami, M.; Mazaheri, F. Single and Binary System Dye Removal from Colored Textile Wastewater by a Dendrimer as a Polymeric Nanoarchitecture: Equilibrium and Kinetics. *J. Chem. Eng. Data* **2010**, *55*, 4660–4668.

(6) Srinivasan, A.; Viraraghavan, T. Decolorization of dye wastewaters by biosorbents: A review. *J. Environ. Manage.* **2010**, *91*, 1915–1929.

(7) Crini, G.; Badot, P. M. Application of chitosan, a natural aminopolysaccharide, for dye removal from aqueous solutions by adsorption processes using batch studies: A review of recent literature. *Prog. Polym. Sci.* **2008**, *33*, 399–447.

(8) Cardoso, N. F.; Lima, E. C.; Calvete, T.; Pinto, I. S.; Amavisca, C. V.; Fernandes, T. H. M.; Pinto, R. B.; Alencar, W. S. Application of Aqai Stalks As Biosorbents for the Removal of the Dyes Reactive Black 5 and Reactive Orange 16 from Aqueous Solution. *J. Chem. Eng. Data* **2011**, *56*, 1857–1868.

(9) Sreelatha, G.; Ageetha, V.; Parmar, J.; Padmaja, P. Equilibrium and Kinetic Studies on Reactive Dye Adsorption Using Palm Shell Powder (An Agrowaste) and Chitosan. *J. Chem. Eng. Data* **2011**, *56*, 35–42.

(10) Mane, V. S.; Mall, I. D.; Srivastava, V. C. Kinetic and equilibrium isotherm studies for the adsorptive removal brilliant green dye from aqueous solution by rice husk ash. *J. Environ. Manage.* **2007**, *84*, 390–400.

(11) Chatterjee, D.; Patnam, V. R.; Sikdar, A.; Moulik, S. K. Removal of Some Common Textile Dyes from Aqueous Solution Using Fly Ash. *J. Chem. Eng. Data* **2010**, *55*, 5653–5657.

(12) Mahmoodi, N. M.; Hayati, B.; Arami, M. Textile Dye Removal from Single and Ternary Systems Using Date Stones: Kinetic, Isotherm, and Thermodynamic Studies. *J. Chem. Eng. Data* **2010**, *55*, 4638–4649.

(13) Dogan, M.; Özdemir, Y.; Alkan, M. Adsorption kinetics and mechanism of cationic methyl violet and methylene blue dyes onto sepiolite. *Dyes Pigm.* **2007**, *75*, 701–713.

(14) Elwakeel, K. Z. Removal of Reactive Black 5 from aqueous solutions using magnetic chitosan resins. *J. Hazard. Mater.* **2009**, *167*, 383–392.

(15) Kyzas, G. Z.; Lazaridis, N. K. Reactive and basic dyes removal by sorption onto chitosan derivatives. *J. Colloid Interface Sci.* **2009**, *331*, 32–39.

(16) Salehi, R.; Arami, M.; Mahmoodi, N. M.; Bahrami, H.; Khorramfar, S. Novel biocompatible composite (Chitosan−zinc oxide nanoparticle): Preparation, characterization and dye adsorption properties. *Colloids Surf., B: Bioint.* **2010**, *80*, 86–93.

(17) Zhou, L.; Jin, J.; Liu, Z.; Liang, X.; Shang, C. Adsorption of acid dyes from aqueous solutions by the ethylenediamine-modified magnetic chitosan nanoparticles. *J. Hazard. Mater.* **2011**, *185*, 1045–1052.

(18) Piccin, J. S.; Vieira, M. L. G.; Gonçalves, J.; Dotto, G. L.; Pinto, L. A. A. Adsorption of FD&C Red No. 40 by chitosan: Isotherms analysis. *J. Food Eng.* **2009**, *95*, 16–20.

(19) Gupta, V. K.; Suhas Application of low-cost adsorbents for dye removal: A review. *J. Environ. Manage.* **2009**, *90*, 2313–2342.

(20) Dotto, G. L.; Pinto, L. A. A. Adsorption of food dyes acid blue 9 and food yellow 3 onto chitosan: Stirring rate effect in kinetics and mechanism. *J. Hazard. Mater.* **2011**, *187*, 164–170.

(21) Weska, R. F.; Moura, J. M.; Batista, L. M.; Rizzi, J.; Pinto, L. A. A. Optimization of deacetylation in the production of chitosan from shrimp wastes: Use of response surface methodology. *J. Food Eng.* **2007**, *80*, 749–753.

(22) Moura, C. M.; Moura, J. M.; Soares, N. M.; Pinto, L. A. A. Evaluation of molar weight and deacetylation degree of chitosan during

chitin deacetylation reaction: used to produce biofilm. *Chem. Eng. Process.* **2010**, *50*, 351–355.

(23) Dotto, G. L.; Souza, V. C.; Pinto, L. A. A. Drying of chitosan in a spouted bed: The influences of temperature and equipment geometry in powder quality. *LWT-Food Sci. Technol.* **2011**, *44*, 1786–1792.

(24) Cervera, M. F.; Heinamaki, J.; Rasanem, M.; Maunu, S. L.; Karjalainen, M.; Acosta, O. M. N.; Colarte, A. I.; Yliruusi, J. Solid state characterization of chitosan derived from lobster chitin. *Carbohydr. Polym.* **2004**, *58*, 401–408.

(25) Dotto, G. L.; Pinto, L. A. A. Adsorption of food dyes onto chitosan: Optimization process and kinetic. *Carbohydr. Polym.* **2011**, *84*, 231–238.

(26) Qiu, H.; Pan, L. L.; Zhang, Q. J.; Zhang, W.; Zhang, Q. Critical review in adsorption kinetic models. *J. Zhejiang Univ. Sci.* **2009**, *A 10*, 716–724.

(27) Wu, F. C.; Tseng, R. L.; Juang, R. S. Characteristics of Elovich Equation Used for the Analysis of Adsorption Kinetics in Dye Chitosan Systems. *Chem. Eng. J.* **2009**, *150*, 366–373.

(28) Cooney, D. O. *Adsorption design for Wastewater Treatment*; Lewis Publishers: New York, 1999.

(29) Crank, J. *The mathematics of diffusion*; Clarendon Press: London, 1975.

(30) Ruthven, D. M. *Principles of Adsorption and Adsorption Processes*; John Wiley & Sons: New York, 1984.

(31) Sakkayawong, N.; Thiravetyan, P.; Nakbanpote, W. Adsorption mechanism of synthetic reactive dye wastewater by chitosan. *J. Hazard. Mater.* **2005**, *145*, 250–255.